AEC DISTRIBUTION FOR PART 50 DOCKET MATERIAL
(TEMPORARY FORM)

CONTROL NO: 5773

FILE

FROM: Wisconsin Public Service Corp. Green Bay, Wis. 54305 E.W. James	DATE OF DOC: 10-18-72	DATE REC'D 10-24-72	LTR X	MEMO	RPT	OTHER
TO: Mr. R.C. DeYoung	ORIG 1 signed	CC 4	OTHER		SENT AEC PDR ✓ SENT LOCAL PDR ✓	
CLASS: U PROP INFO	INPUT	NO CYS REC'D 5			DOCKET NO: 50-305	

DESCRIPTION: Ltr re our 10-4-72 ltr....trans the following:

ENCLOSURES: Addl Info re Containment Pressure Response to LOCA.....

(5 cys encl rec'd)

PLANT NAMES: Kewaunee Plant

DO NOT REMOVE **ACKNOWLEDGED**

FOR ACTION/INFORMATION
DL 10-25-72

BUTLER(L) W/ Copies	SCHWENCER(L) W/ Copies	SCHEMEL(L) W/ Copies	KNIGHTON(ENVIRO) W/ Copies
CLARK(L) W/ Copies	STOLZ(L) W/ Copies	ZIEMANN(L) W/ Copies	YOUNGBLOOD(ENVIRO) W/ Copies
GOLLER(L) W/ Copies	VASSALLO(L) W/ Copies	CHITWOOD(FM) W/ Copies	REGAN(ENVIRO) W/ Copies
✓ KNIEL(L) W/ 6 Copies	H. DENTON W/ Copies	DICKER(ENVIRO) W/ Copies	W/ Copies

INTERNAL DISTRIBUTION

✓ REG FILE	TECH REVIEW	✓ VOLLMER	HARLESS	WADE E
✓ AEC PDR	✓ HENDRIE	DENTON		SHAFER F & M
✓ OGC, ROOM P-506A	✓ SCHROEDER	GRIMES	F & M	BROWN E
✓ MUNTZING/STAFF	✓ MACCARY	GAMMILL	SMILEY	G. WILLIAMS E
✓ CASE	✓ LANGE	KASTNER	NUSSBAUMER	E. GOULBOURNE L
GIAMBUSSO	✓ PAWLICKI	BALLARD		A/T IND
BOYD-L(BWR)	✓ SHAO	FINE	LIC ASST.	BRAITMAN
✓ DEYOUNG-L(PWR)	✓ KNUTH		SERVICE L	SALTZMAN
✓ SKOVHOLT-L	✓ STELLO	ENVIRO	MASON L	
P. COLLINS	✓ MOORE	MULLER	WILSON L	PLANS
	✓ HOUSTON	DICKER	MAIGRET L	MCDONALD
REG OPR	✓ TEDESCO	KNIGHTON	SMITH L	DUBE
✓ FILE & REGION (2)	✓ LONG	YOUNGBLOOD	GEARIN L	
✓ MORRIS	✓ LAINAS	PROJECT LEADER	DIGGS L	INFO
✓ STELLE	✓ BENAROYA		TEETS L	C. MILES
		REGAN	LEE L	

EXTERNAL DISTRIBUTION

✓ 1-LOCAL PDR Kewaunee, Wis.
✓ 1-DTIE(ABERNATHY)
✓ 1-NSIC(BUCHANAN)
1-ASLB-YORE/SAYRE WOODWARD/H. ST.
✓ 16-CYS ACRS HOLDING

(1)(5)(9)-NATIONAL LAB'S
1-R. CARROLL-OC, GT-B227
1-R. CATLIN, A-170-GT
1-CONSULANT'S NEWMARK/BLUME/AGABIAN

1-PDR-SAN/LA/NY
1-GERALD LELLOUCHE BROOKHAVEN NAT. LAB
1-AGMED(WALTER KOESTER, Rm C-427, GT)
1-RD...MULLER...F-309GT

Regulatory File Cy.

WISCONSIN PUBLIC SERVICE CORPORATION

P.O. Box 1200, Green Bay, Wisconsin 54305

Docket No. 50-305

October 18, 1972

RECEIVED
OCT 24 1972
U.S. ATOMIC ENERGY COMMISSION
Regulatory Mail Section

Mr. R. C. DeYoung, Assistant Director
for Pressurized WAter Reactors
Division of Reactor Licensing
U. S. Atomic Energy Commission
Washington, D. C. 20545

Dear Mr. DeYoung:

Subject; Request for Additional Information
Your Letter of October 4, 1972

In your letter of October 4, you state that you need additional information to evaluate reactor containment building pressure during loss of coolant accidents as well as the response of reactor building compartment walls during such events. This information is being submitted as an attachment to this letter.

Very truly yours,

E. W. James

E. W. James, Senior Vice President
Power Generation and Engineering

EWJ:mem
Attach.
cc - Mr. Steven E. Keane
Foley & Lardner

Mr. Gerald Charnoff
Shaw, Pittman, Potts, Trowbridge & Madden

DOCKETED
USAEC
OCT 24 1972
REGULATORY
MAIL SECTION
DOCKET CLERK

5773

QUESTION 5.85

Provide the following information. All assumptions used in the analysis should be explained. Assumptions should be conservative with respect to the calculation of containment pressures.

QUESTION 5.85.1

Containment pressure-time response analyses should be provided for selected design basis loss-of-coolant accidents. Double-ended breaks of the largest reactor outlet pipe and double-ended breaks of the reactor coolant pump suction and discharge pipes should be included. Smaller pipe breaks should also be analyzed and should be selected to be representative of the spectrum of break sizes for both inlet and outlet reactor coolant pipes. The analyses should be extended, as a minimum, through the blowdown, reflood and post-reflood phases of the accidents (i.e., for about 1. hour following the accident).

QUESTION 5.85.2

The reflood model that is used following blowdown should be described in detail. The description should include the assumptions used to develop the model, e.g., hydraulic modeling of the primary coolant system, resistances of components (primary coolant pump, steam generator, piping and reactor core), and the methods used in computing steam generation in the core and other energy sources (core stored energy, decay heat [short and long term] thick and thin metal-stored energy, and steam generator-stored energy).

QUESTION 5.85.3

If the blowdown model differs from that described in the SAR for containment calculations, the differences should be discussed in detail.

QUESTION 5.85.4

For the cold leg break, the size and location resulting in the highest calculated containment pressure analyzed in Item 1, tables of mass release (pounds/second), the enthalpy of the mass (BTU/pound) released from the core, and the mass and enthalpy released to the containment should be provided throughout the blowdown and reflood phases of the accident. A graph showing core inlet velocity as a function of time should also be provided for the reflood phase of the accident.

Note:

Answers to the above questions have been consolidated and are contained in the discussion that follows.

CONTAINMENT PRESSURE RESPONSE TO LOCA

Received w/Ltr Dated 10-18-72

The containment pressure response has been analyzed considering the steam generators as an active heat source during reflood. The analysis presented is for the double ended guillotine pump suction break which has been found to be the most conservative. In addition, sensitivity studies are presented to show the containment pressure transient as a function of break size and location.

The calculational model may be divided into three parts: Blowdown, when the system pressure drops from 2250 psia to containment pressure; Refill, when the vessel inventory is increased to the bottom of the core; and Reflood, where the water level moves into the core.

BLOWDOWN The model for blowdown is essentially the same as that used in the FSAR containment analysis. The SATAN code is used to simulate breaks in the various locations. All accumulators inject for breaks other than the cold leg. One difference in the calculational model is that the steam generator heat transfer during blowdown now accounts properly for the heat transfer coefficient on the shell (secondary) side when heat flow is from secondary to primary. Previously this value was maintained at the high initial value, thus allowing an exceedingly high heat flow from the secondary to the primary side of the steam generators. In the present model the heat transfer coefficient on the shell side when heat flow is from secondary to primary is calculated using McAdam's recommendation for turbulent boundary layers on vertical surfaces. Also, the initial fluid energy contained in the primary system has been adjusted slightly to properly reflect the correct system volume plus appropriate margin.

The previous SATAN initial stored energy in the core has been identified as being exceedingly conservative. A more accurate value which includes appropriate conservatism is used here. The amount of heat released from the core over blowdown had been studied and an upper bound had been determined by a suitably conservative analysis. Specifically, an average channel heat release analysis was performed using the LOCTA code. The transition boiling correlation and DNB time were modified to obtain a conservatively high release rate. The resulting upper bound value is used in the present analysis.

REFILL The calculations in this period have been minimized by making the conservative assumption that the bottom of core recovery occurs immediately after the end of blowdown.

DESCRIPTION OF THE CORE REFLOODING MODEL

The SATAN calculations are performed until the completion of blowdown. In this context the end of blowdown is defined as the time at which zero break flow is first computed. At this time, the normal blowdown transient calculations are terminated and the reflooding calculations are performed. The reflooding model consists of three reference volumes which represent the downcomer region, the lower plenum region, and the active core region. The core and the downcomer volumes both communicate with the lower plenum volume via non-resistive flow paths. An input containment backpressure is assumed to act directly on the top of the downcomer volume, and any steam generated in the core region is vented to the containment via a flow path whose resistance simulates the flow path to the break. The model is shown in Figure 1. Provisions for heat transfer from vessel walls and reactor internals to injection water are also included in this model.

When the bottom of the core is reflooded by the accumulator water, steam is generated by the hot fuel rods, causing a pressure build-up in the core region. This retards the core reflooding process. The steam generated must be vented from the system through the break, and the flooding rate is limited by the resistance of the loop to the steam and water flow. There are two paths available for the steam and entrained water flow to the break. The first path is directly to the break through the broken loop. The other path is through the intact loops, back into the inlet annulus, and finally to the break through the inlet nozzle in the broken leg. These flow paths, as depicted in Figures 2 and 3, show the path the steam must follow for the cold-leg break. The pressure drops along these two paths are calculated with the existing fluid conditions and associated loss coefficients. The pressure drop across the pump is calculated by assuming that the rotor is free spinning. In addition, it is postulated that the accumulator water injected plus the pumped injection is sufficient to maintain the downcomer full with the high calculated flooding rates. No plugging of the cold leg pipe during accumulator injection was assumed. These assumptions tend to increase the core flooding rate and the containment energy release, thus resulting in increased peak containment pressure. In the present analysis, no credit is taken for the quenching of the effect of the injection water that does not enter the core.

The amount of mass vaporized and entrained as a function of core flooding rate and time after reflooding is obtained from an analysis of the FLECHT results. These results indicate that several flow regimes are present in the rod bundle during reflooding. For the first few seconds of the reflooding transient, until the core floods to approximately 20 inches, most of the heat transferred from the rod to the coolant goes to increase the liquid enthalpy. During this period almost no steam generation takes place and the core flooding rate equals the cold flooding rate. Following this initial period the steam velocity increases above the value required for entrainment and a dispersed flow regime begins. This flow pattern is characterized by a continuous vapor phase with dispersed droplets and by a fast increase in rod heat transfer coefficient.

It is during this phase of the reflooding transient that the flooding rate into the core is determined by the resistance of the flow paths from the core to the break. The core flooding rate transient during this period is a function of the core and loop resistance, the fraction of coolant vaporized and entrained, and the difference in water level between the downcomer and the core. The fraction of coolant vaporized, entrained and leaving the core is not constant during the transient, but increases from zero at the beginning to 70 to 80 percent of the entering coolant several seconds after initiation of reflooding depending on the core flooding rate. This is supported by FLECHT data. The Westinghouse proprietary entrainment correlation, presented in the ECCS rulemaking proceedings, has been used to evaluate the amount of mass leaving the top of the core as a function of time. The model is over conservative in that fall back in the upper plenum is expected. Study of this effect is continuing. These assumptions are conservative because they result in an extremely high flooding rate.

From FLECHT data, it is found that entrainment begins after the level in the core rises 20 inches. It continues until the entire core is quenched. The FLECHT data shows that by the time the 8 ft. elevation is quenched by the rising water level, the 10 ft. elevation has already been quenched. This is shown in Figure-4. In the present analysis, it has been conservatively assumed that entrainment continues until the quench front reaches the 8 ft. elevation. The sensitivity of this assumption is evaluated by sensitivity studies.

An energy balance is performed on the fluid entering and leaving the core in order to determine core exit quality. For the purposes of this calculation, core stored and thin metal energy are brought out at a constant rate over the period between bottom of core recovery and the quench of 8 ft. elevation. Decay heat is brought out as produced and thick metal energy decays exponentially.

The flow split between unbroken loop and broken loop steam generators is based on appropriate resistance considerations. Fluid which enters the steam generator tube side is assumed to be heated instantaneously to the shell side temperature. This heat flow results in a reduction in shell side temperature over the course of reflood. The superheated fluid then flows into the containment. For hot leg breaks the flow that leaves the core is subdivided between the direct flow to the break and that to the unbroken loop, vessel annulus and broken loop path. Only the latter is superheated in the steam generator. The former is discharged to the containment at the core exit conditions.

Results

The analysis described above has been performed. The mass and energy released to the containment as a function of time is given in Figures 5, 6 and 7. This results in the containment pressure transient given in Figure 9. For this case the core inlet velocity as a function of time after bottom of core recovery is given in Figure 8. The peak pressure for the design case is 42.7 psig.

In addition to the above case, the following cases were considered to determine the sensitivity of the pressure transient to various inputs. For these calculations the additional blowdown thin metal energy release and entrainment up to the 10 foot level were considered.

Figure 10 gives the Containment Pressure Transient for the Double Ended Guillotine Pump Suction Break.

Figure 11 is for the 0.6 Double Ended Guillotine Pump Suction Break.
Figure 12 is for the 3.0 ft^2 Pump Suction Break.
Figure 13 is for the Double Ended Guillotine Hot Leg Break.
Figure 14 is for Double Ended Guillotine Pump Discharge Break.

This information will be further documented as required.

TABLE 1

ENERGY FROM TOP OF CORE VS TIME

Time (Seconds)	mh at core exit (BTU/sec)	mh to containment (BTU/sec)	Temp. of Steam Genereator in Broken Loop	Temp. of Steam Generator in unbroken Loop
12.8	267,000	190,000	493.4°F	509.0°F
16.4	313,300	317,900	494.0	509.7
18.8	307,150	419,100	493.7	509.5
50.0	230,800	388,900	481.0	502.0
75.0	214,700	367,400	470.0	496.0
100.0	204,880	347,100	460.0	490.0
150.0	187,900	303,100	441.0	480.0

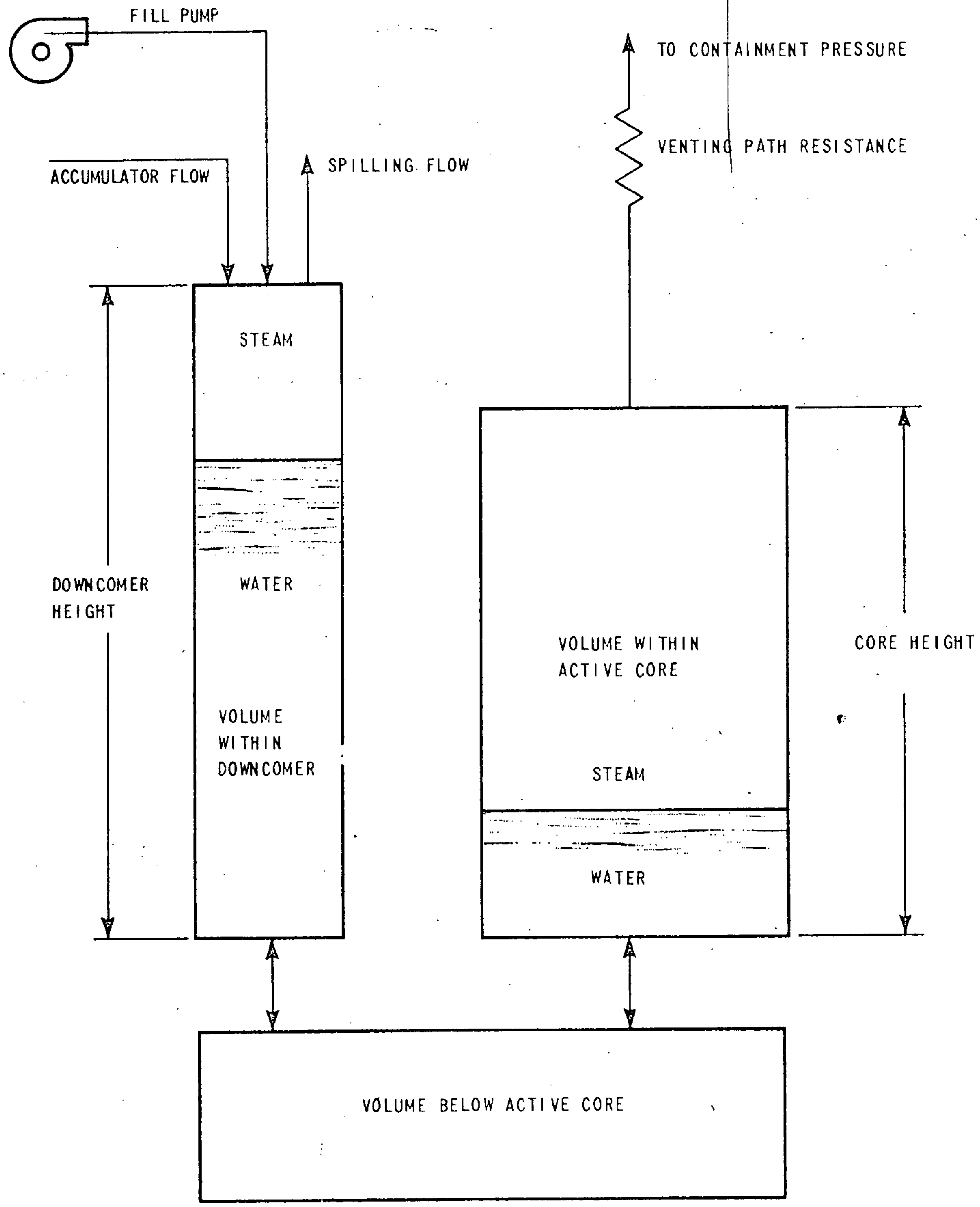

Figure 1 Block Diagram for Satan-V Refill Calculation

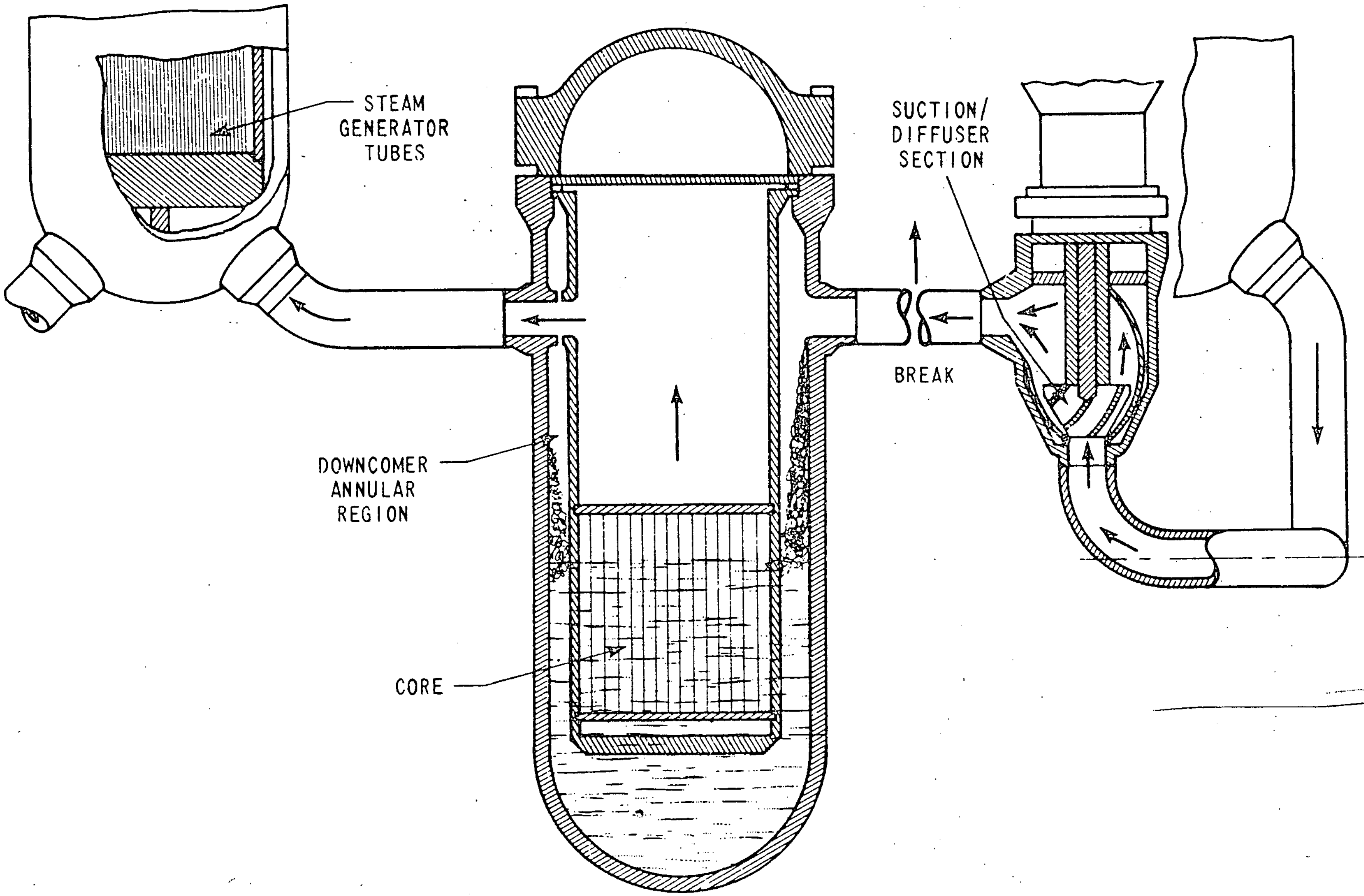

Figure -2
COLD LEG BREAK STEAM FLOW PATH SCHEMATIC

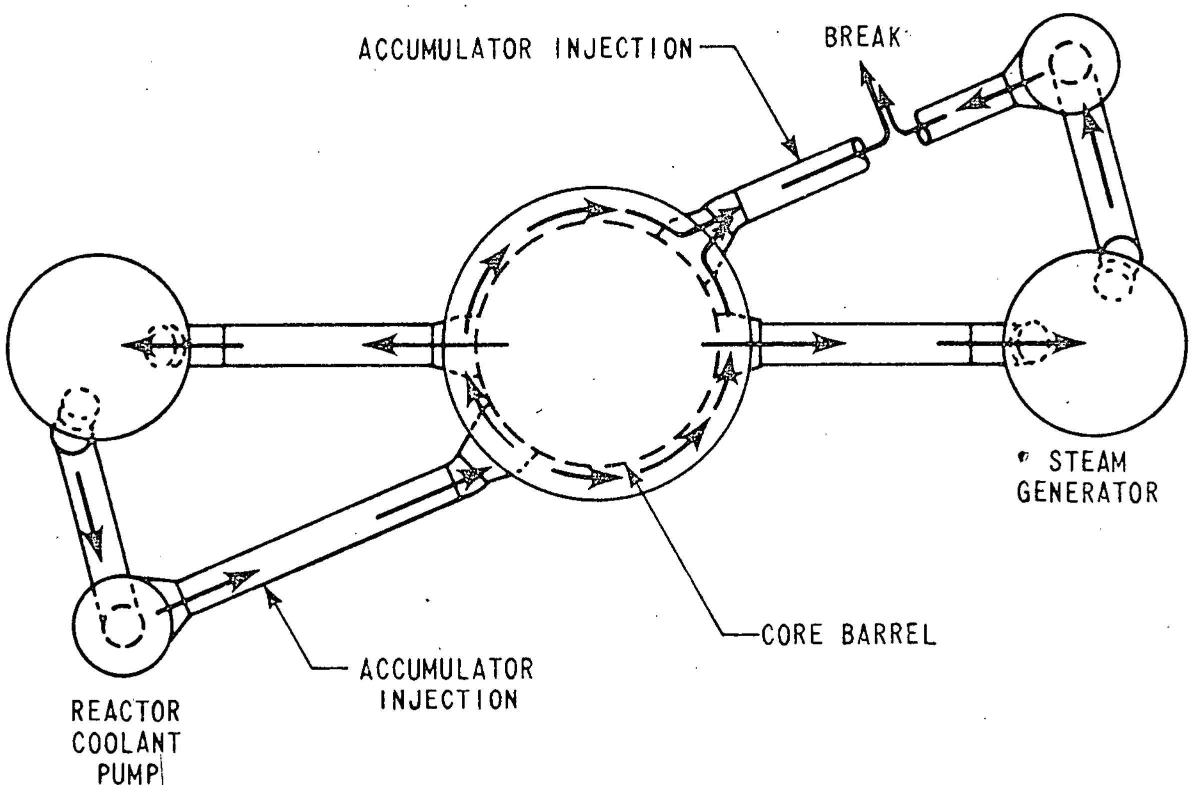

Figure -3

COLD LEG BREAK STEAM FLOW PATH SCHEMATIC

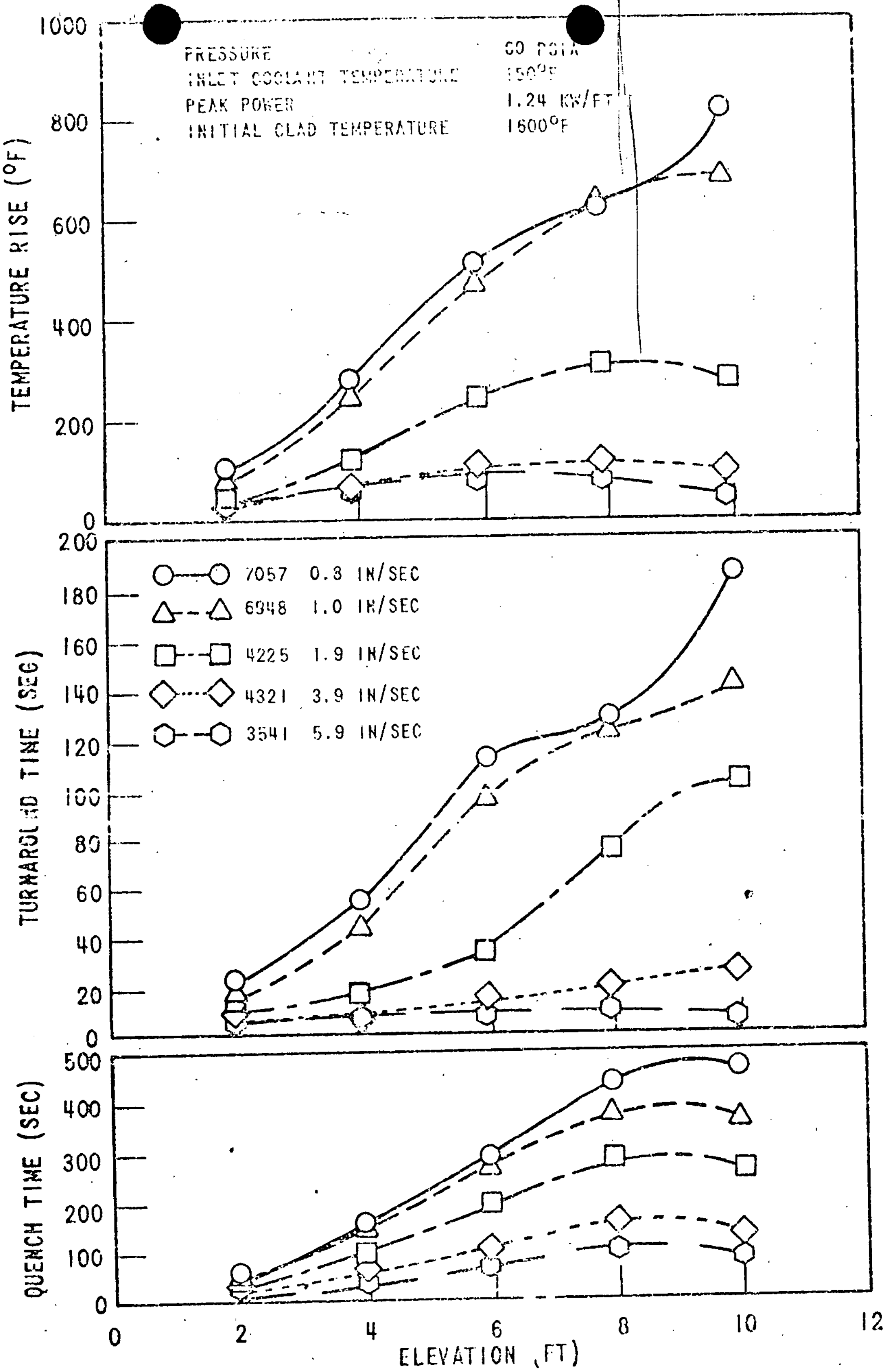

Figure -4 Variation in Temperature Rise, Turnaround Time, and Quench Time with Elevation

K+E 10 X 10 TO ½ INCH 46 1320
7 X 10 INCHES MADE IN U.S.A.
KEUFFEL & ESSER CO.

Figure -5

Double Ended Crossover Break

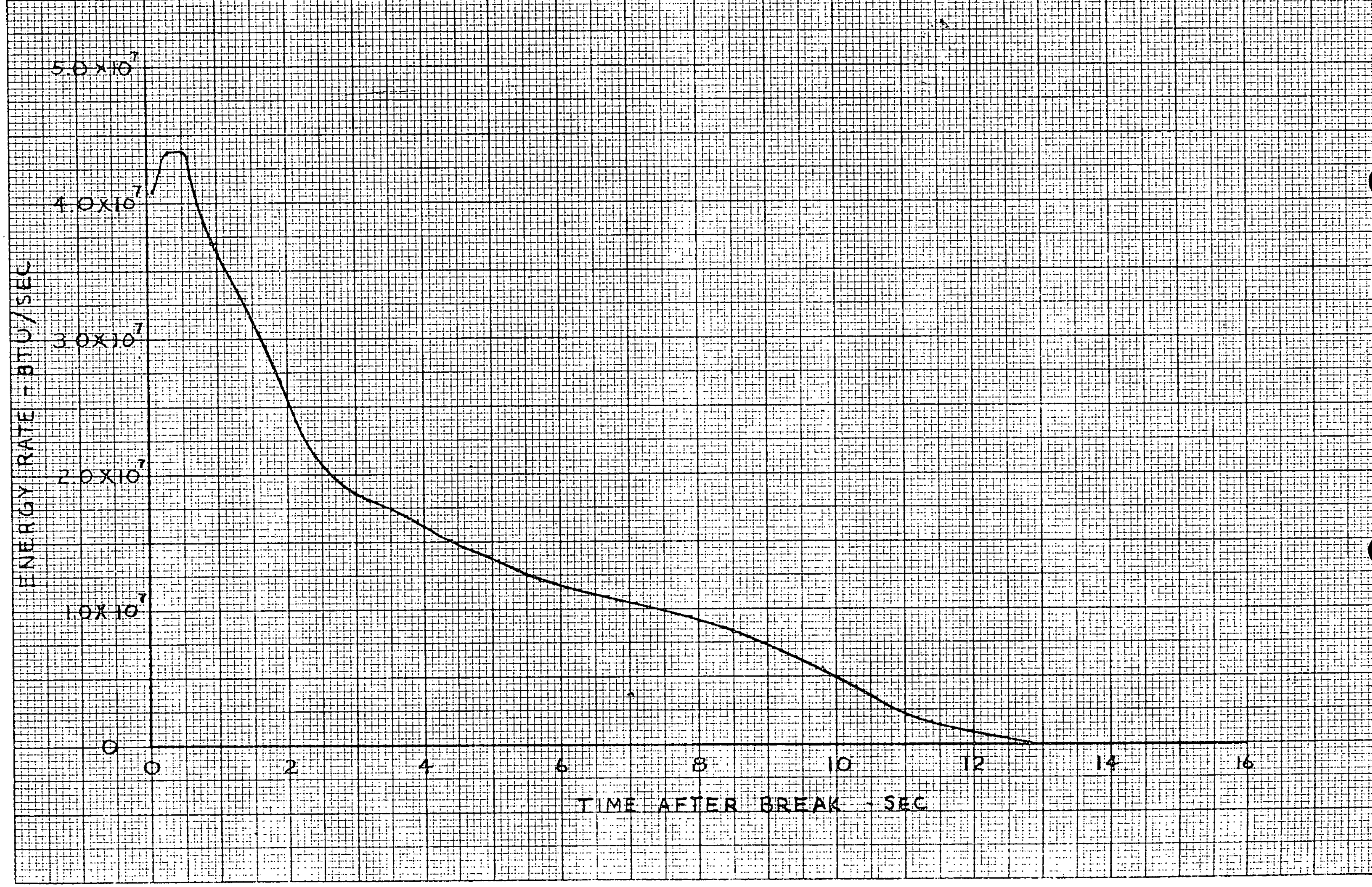

Figure -6

Double Ended Crossover Break

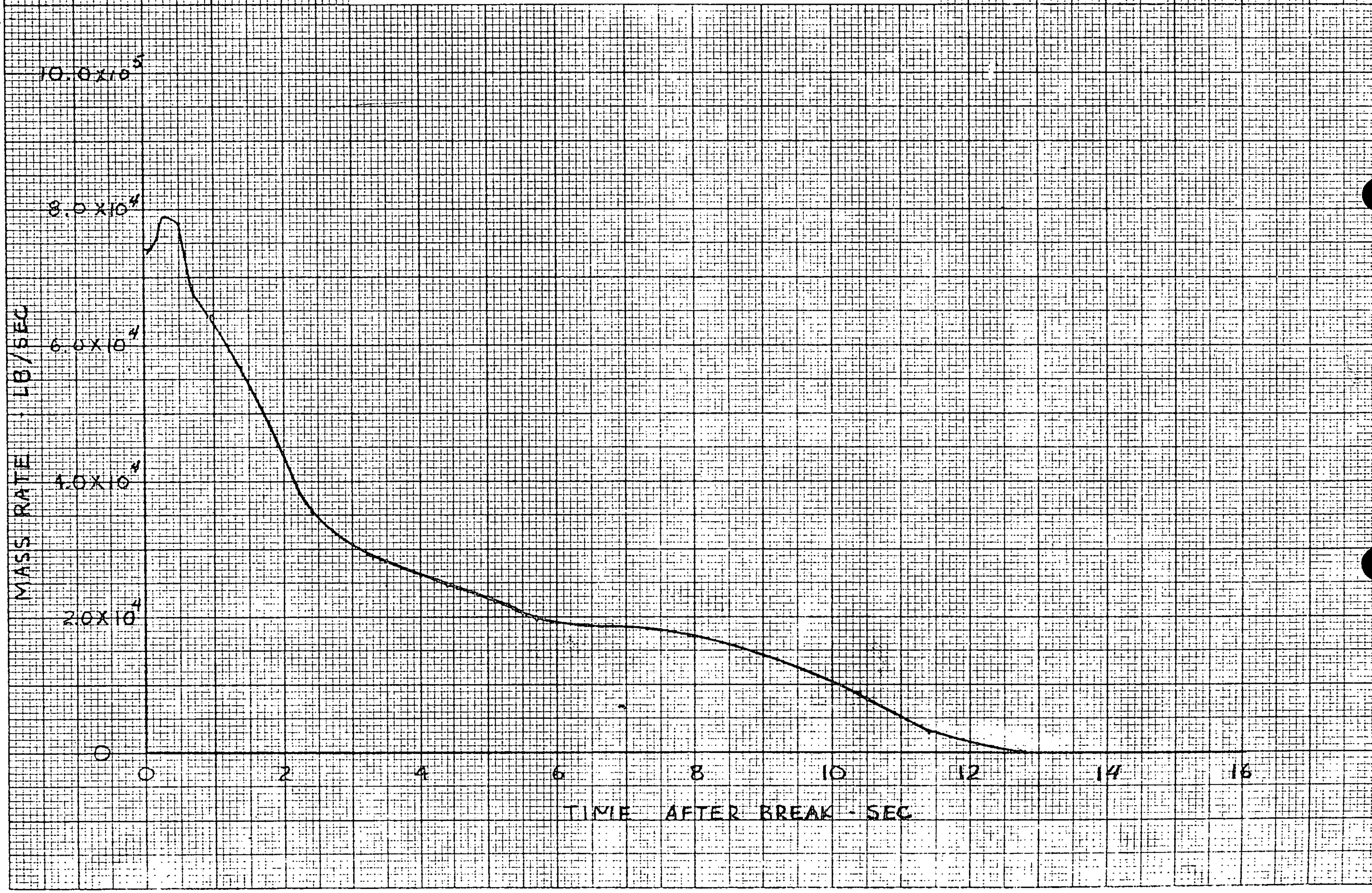

Figure -7
Double Ended Pump Suction Break

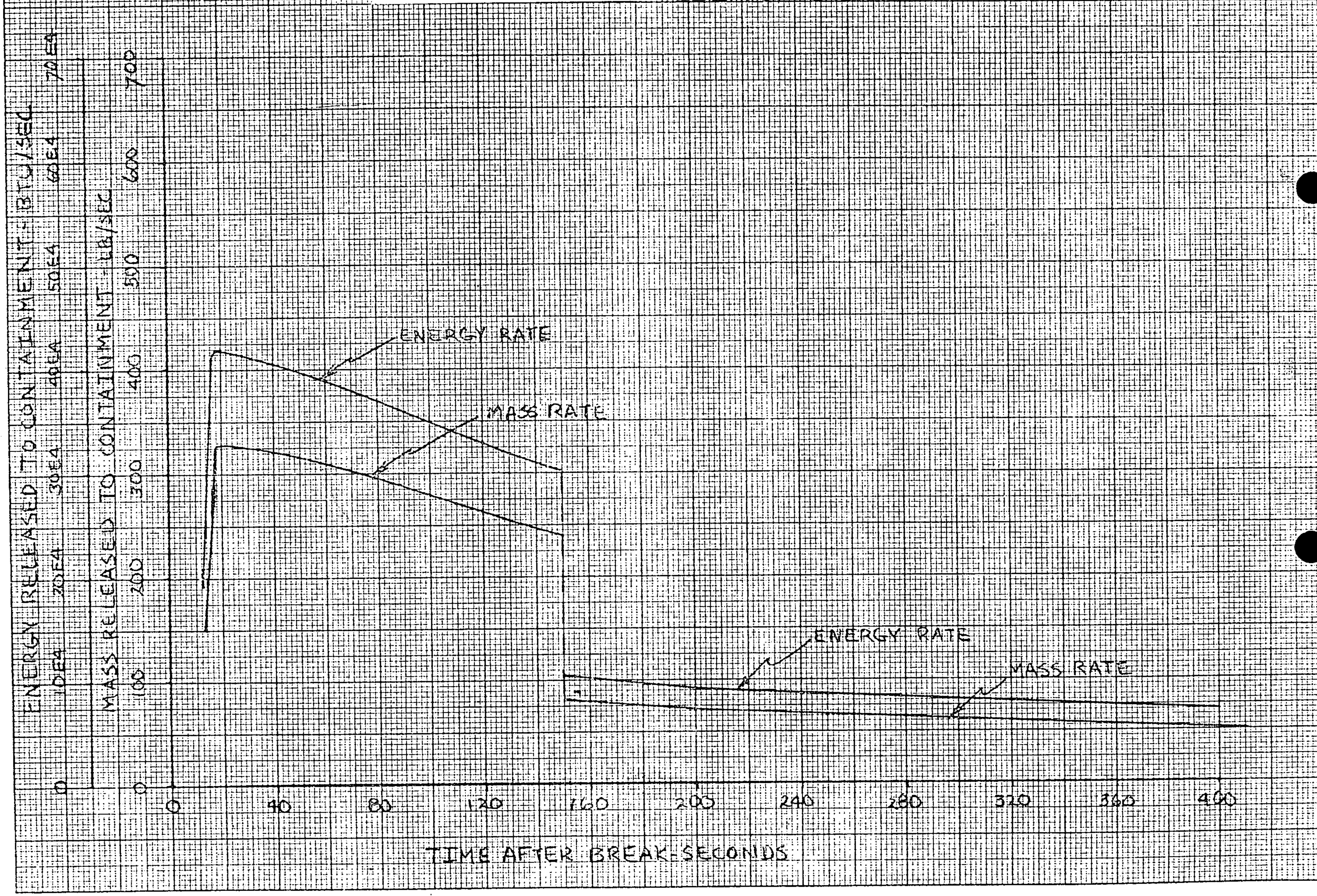

Figure -8

Double Ended Crossover Break

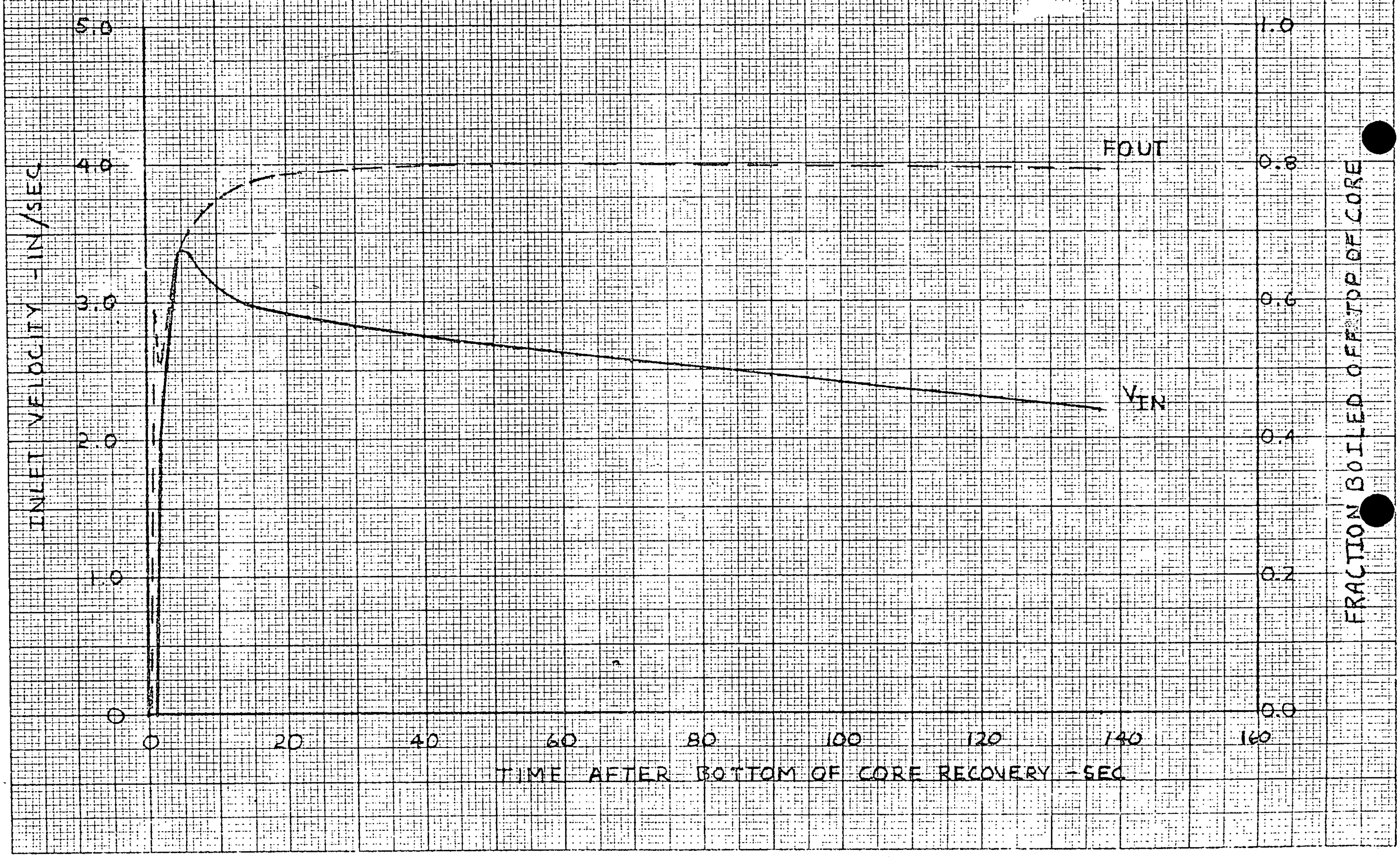

Figure -9

Double Ended Pump Suction Break

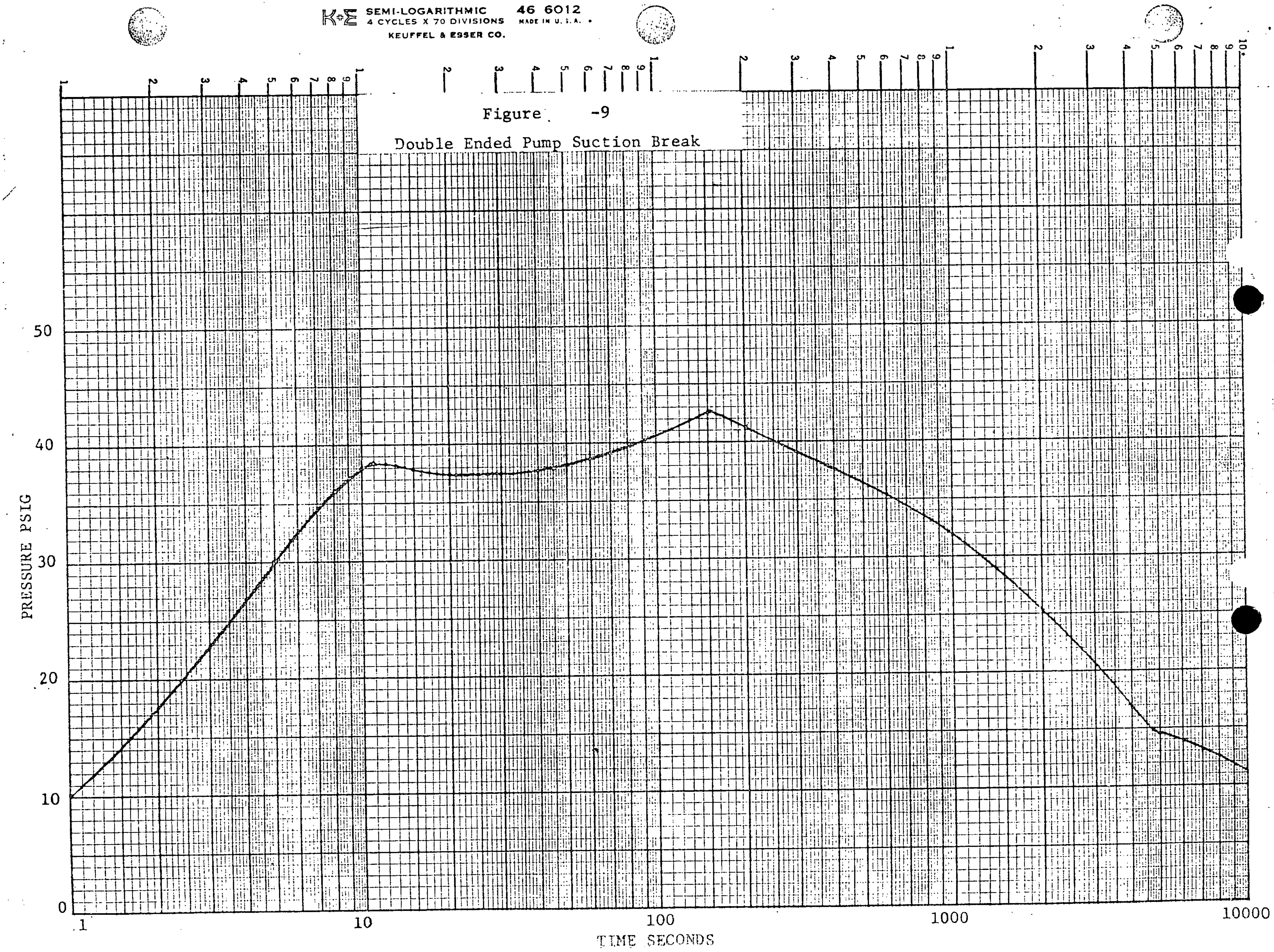

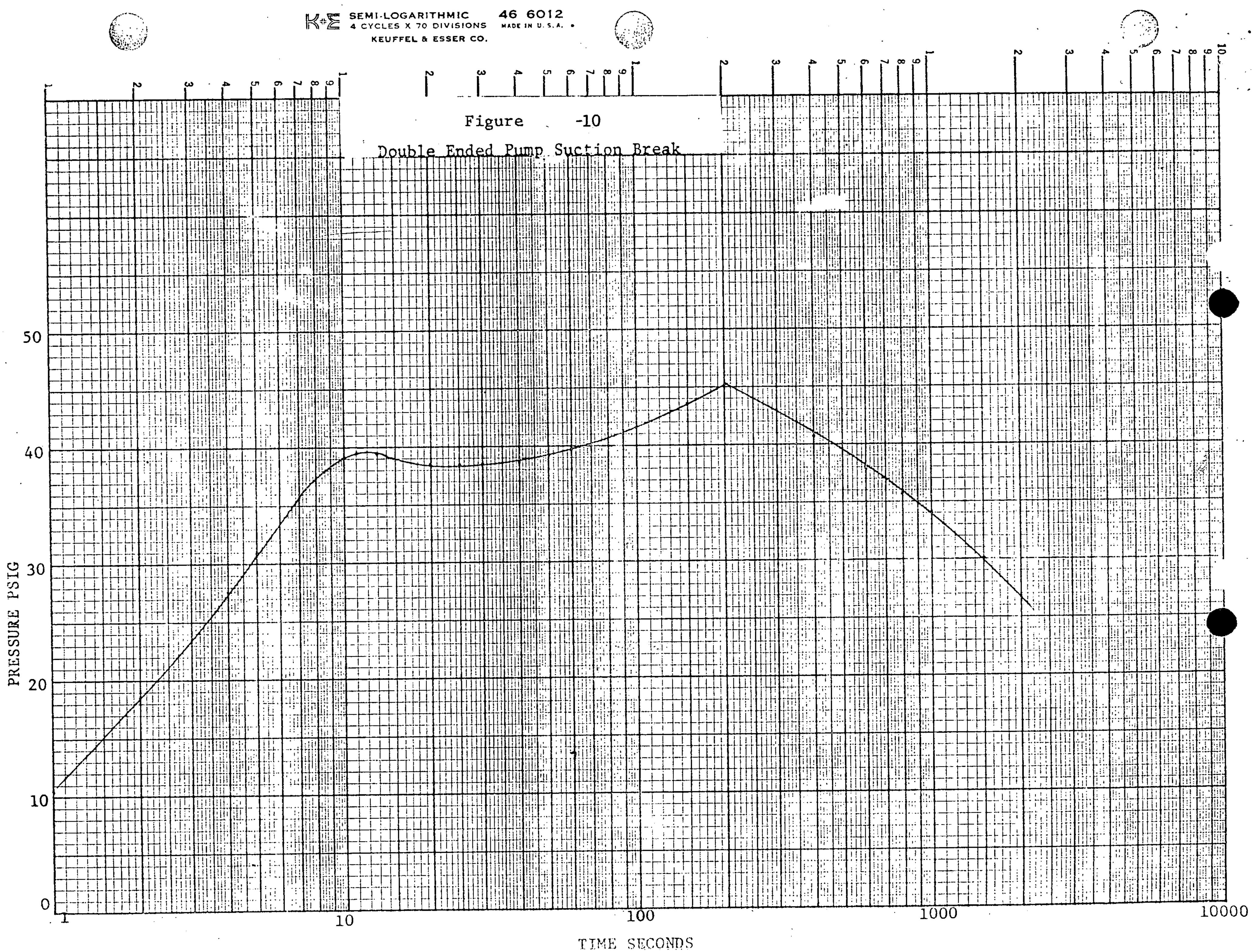
K+E SEMI-LOGARITHMIC 4 CYCLES X 70 DIVISIONS
KEUFFEL & ESSER CO.
46 6012 MADE IN U.S.A.
Figure -10
Double Ended Pump Suction Break
PRESSURE PSIG
50
40
30
20
10
0
1
10
100
1000
10000
TIME SECONDS

Figure 11

.6 Double Ended Pump Suction Break

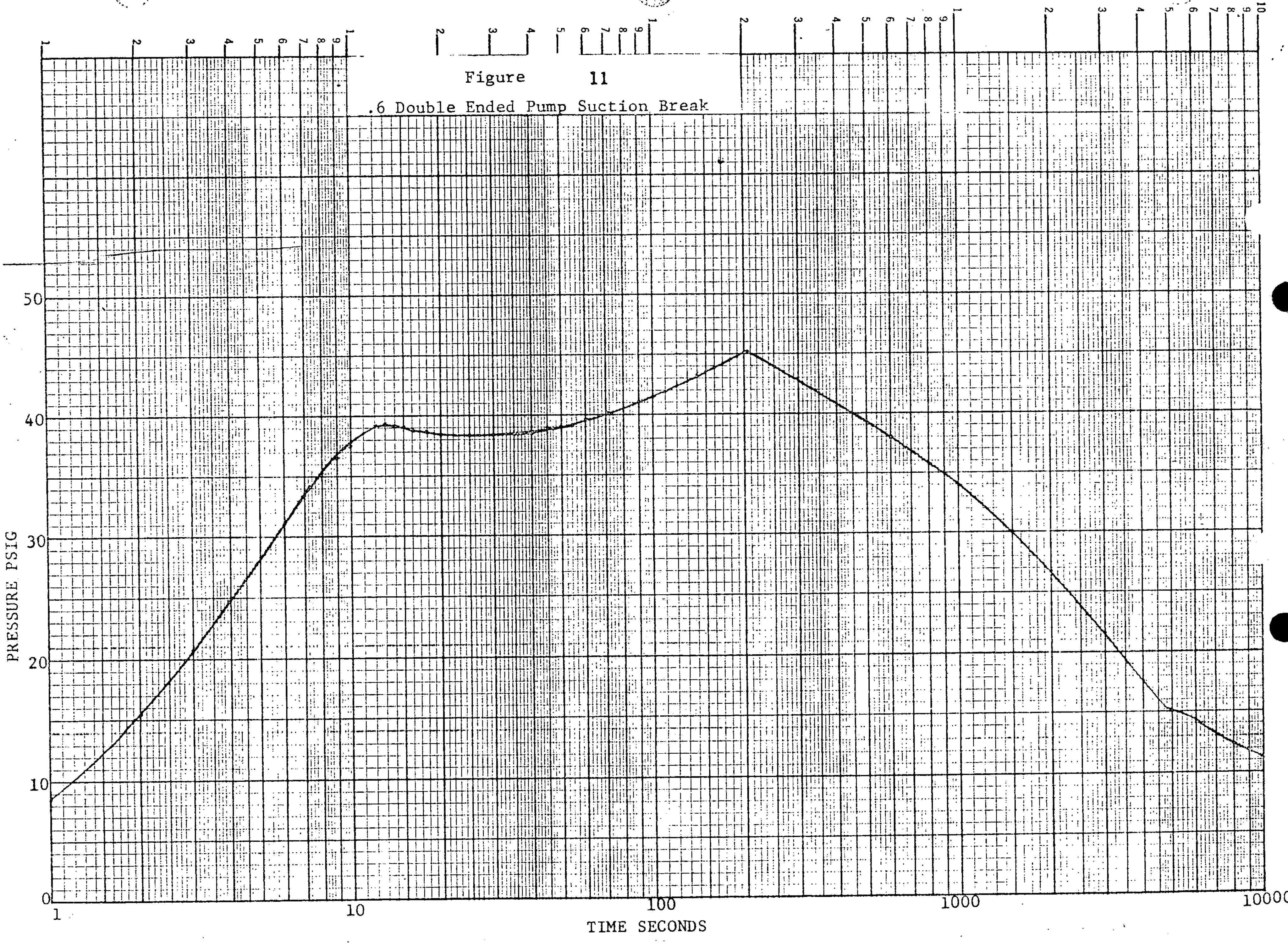

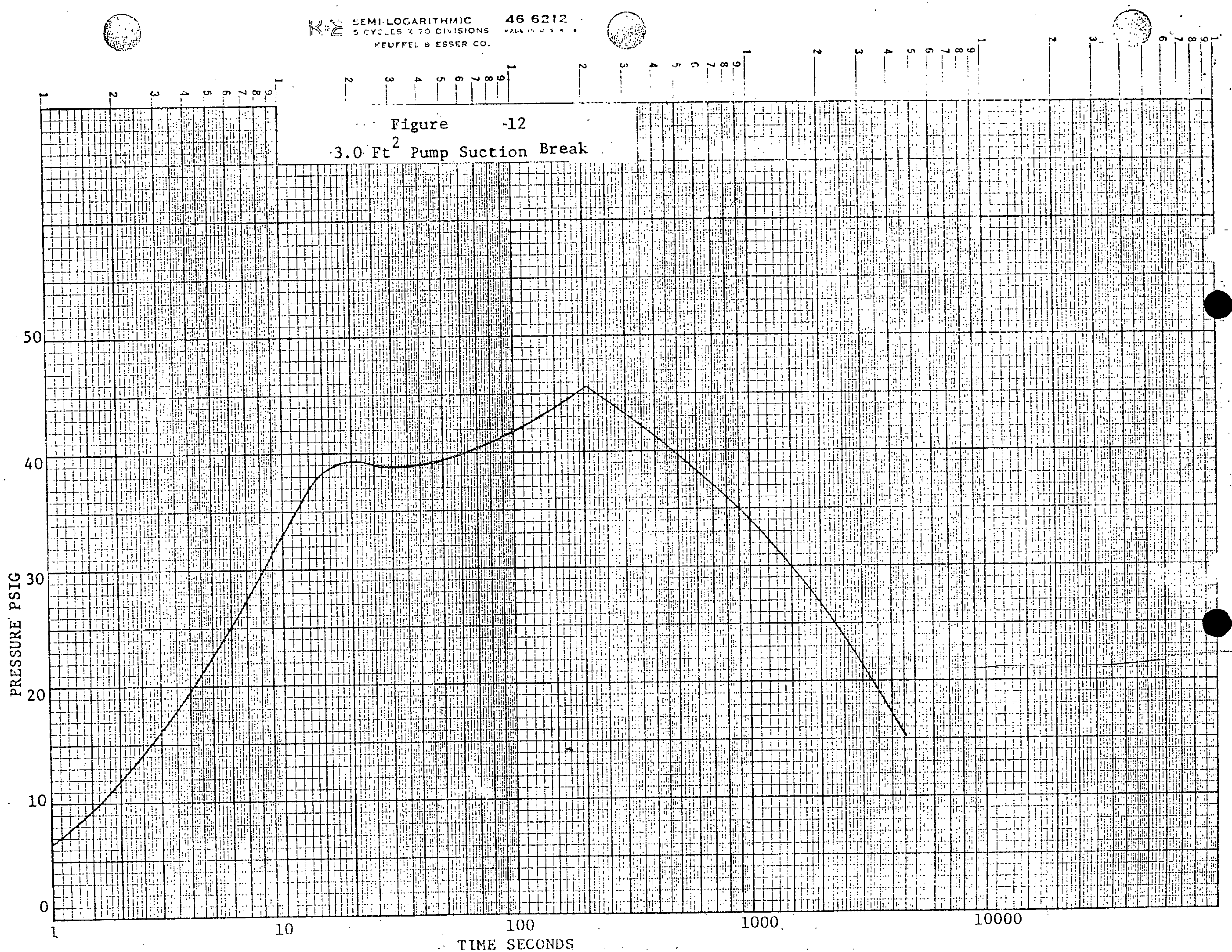

Figure -12

3.0 Ft^2 Pump Suction Break

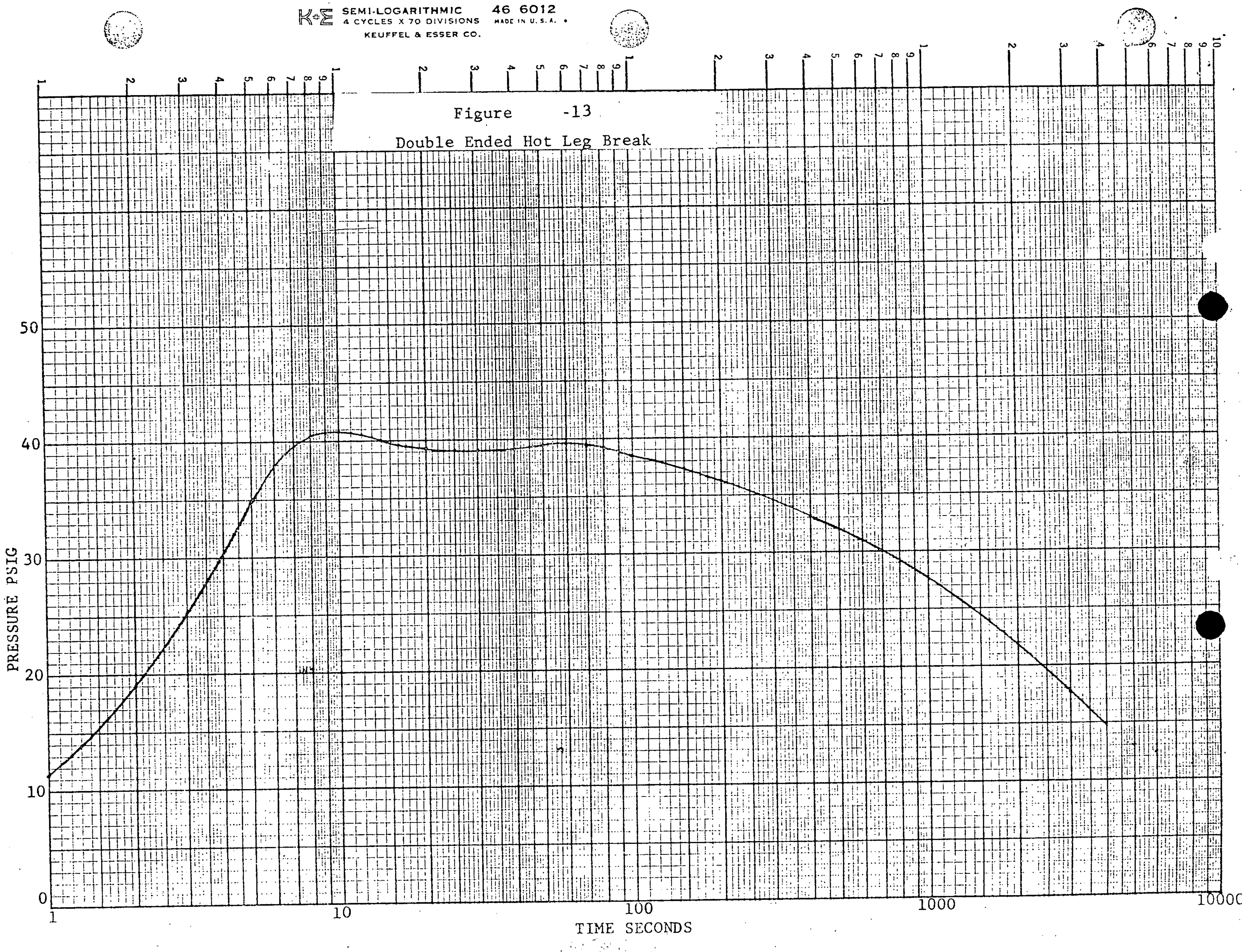

Figure -13
Double Ended Hot Leg Break

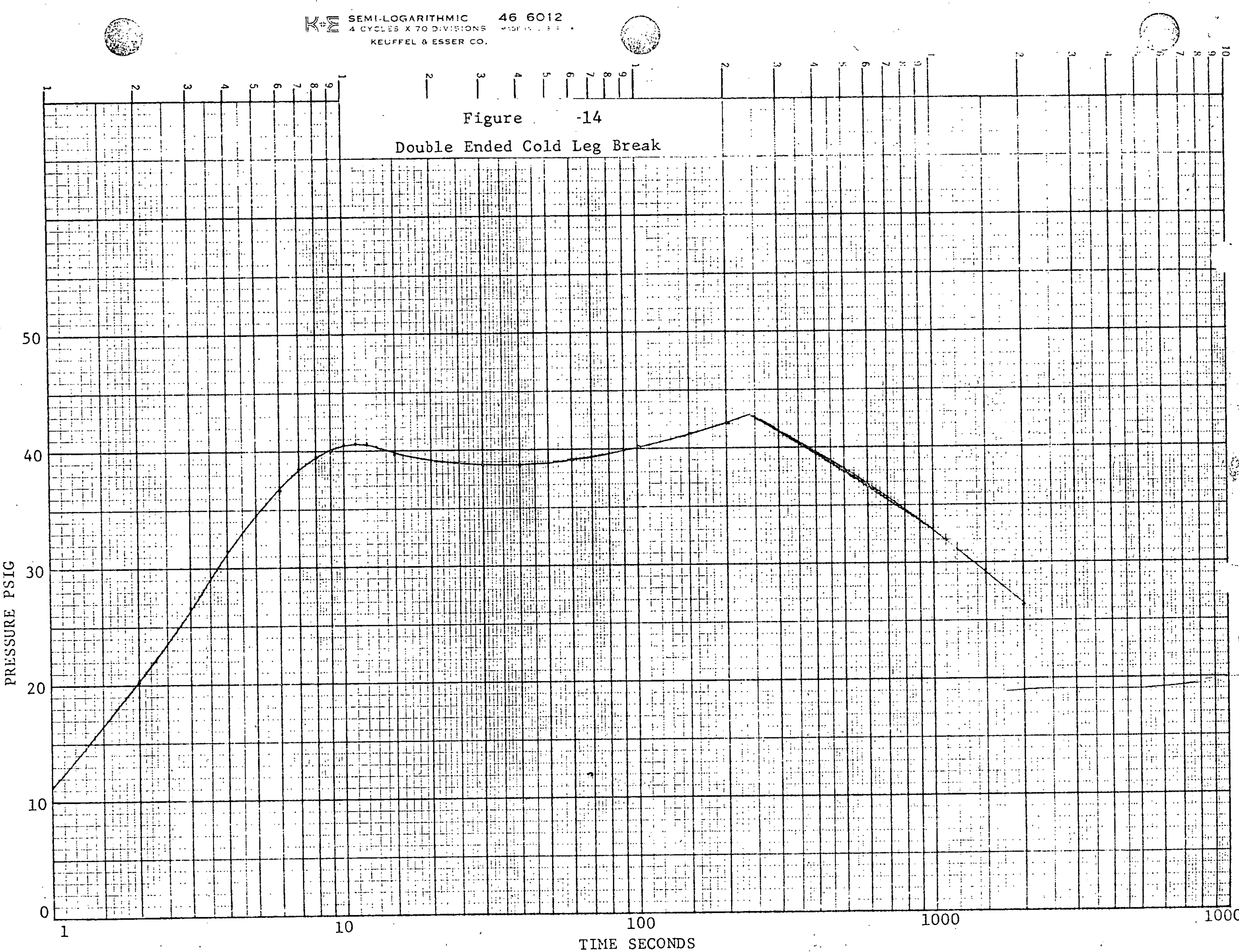

K+E SEMI-LOGARITHMIC 46 6012
4 CYCLES X 70 DIVISIONS
KEUFFEL & ESSER CO.
Figure -14
Double Ended Cold Leg Break
PRESSURE PSIG
0
10
20
30
40
50
1
10
100
1000
10000
TIME SECONDS

QUESTION 5.86

With regard to reactor building compartment differential pressure analyses:

QUESTION 5.86.1

Identify the reactor building compartments analyzed. Provide the reactor coolant system break size and the free volume and vent area for each compartment.

QUESTION 5.86.2

Describe the analytical model used to perform the analyses and discuss the assumptions in the model, including moisture carryover and the time steps used in predicting pressure differentials across compartment walls.

QUESTION 5.86.3

Discuss the results of the analyses performed for each compartment, including the maximum absolute and differential pressures attained, and the jet forces on the compartment walls.

QUESTION 5.86.4

Discuss the structural design capability of each compartment to withstand the differential pressure and jet forces resulting from loss-of-coolant accidents for each compartment.

Note:

Answers to the above questions have been consolidated and are contained in the discussion that follows.

COMPARTMENT DIFFERENTIAL PRESSURE ANALYSIS

Compartments and Break Sizes

The reactor building compartments considered in the differential pressure analysis are the steam generator vaults, the base compartments, foundation void, penetration annuli, reactor vessel gap and the tube tunnel. Sketches of compartment locations are shown in Figure 1 and Figure 2, and the associated volumes and opening areas are given in Tables 1 and Table 2.

The analysis of the steam generator vaults and connecting compartments (see Figure 1.) used a 3ft.^{2} pump suction break. Analysis of the nozzle annuli and reactor vessel gap (see Figure 2.) used the initial mass and energy flow rate values of the 3 ft.^{2} pump suction break because the initial flow rates were the maximum values.

Analytical Model

A computer program was used to determine the pressure for the steam generator vaults and adjacent compartments, and hand calculations were used to determine the penetration annuli and reactor vessel gap pressures.

In the compartment pressure computer code the vault where pipe rupture occurs has mass and energy input flowrates based on the flowrates from the reactor system blowdown code. (Figure 3.) The initial conditions of each vault are identical to those of the bulk containment; namely 120°F and 14.7 psia. A sequence of calculations are performed to determine the mass and energy transferred between compartments for a short time interval (10 msec) and to compute the resulting compartment pressures. The time interval was carefully selected to assure the solution for compartment pressure transients converged. The sequence begins by evaluating the mass and energy input rates to the rupture vault at the midpoint of a time interval and adding these increments to the current amounts in the rupture vault. An intermediate state is then obtained by applying energy and mass balance equations to the total contents of the rupture vault. No discharge or outflow is assumed to take place at this intermediate phase of the calculation.

Analytical Model (Continued)

This intermediate state in the rupture vault and the adjacent compartment conditions at the beginning of the time interval along with the flow geometry, determine the amount of steam and air to be discharged to adjacent compartments. The final state of the rupture vault, after a portion of steam and air has been discharged, is obtained again by an energy and mass balance. The same calculational procedures are repeated for each adjacent compartment. The results of the compartment pressure analysis are shown in Figure 4. Of the two steam generator vaults, the one with the smaller volume and exit area was used in the analysis, because it would result in the highest pressures.

Hand calcualtions were used to compute the pressures of the reactor nozzle cavity and the reactor vessel gap, since these are more likely to function as flow passages rather than reservoirs due to the high ratio of escape area to net volume. Conservatively, a steady state blowdown rate equal to the initial (also the maximum) blowdown rate of the 3 ft.^{2} pump suction break was used. From blowdown calculations the initial mass flow rate is 76,000 lbm/sec and the blowdown energy is 560 btu/lbm. The cavity surrounding the reactor vessel nozzle opening (117.3 ft.^{3}) has the smallest discharge area (23.5 ft.^{2}), and hence will be subject to the highest pressure. Using a two-phase steady-state critical flow analysis (the Moody correlation) the 76,000 lbm/sec flowrate (where stagnation enthalphy is 560 Btu/lbm) requires a driving potential of 475 psia to escape from the cavity. The peak absolute pressure is thus 475 psia with a maximum differential compartment pressure of 475-14.7 = 461.3 psi. The same analysis was used to compute the pressures in the reactor vessel gap, assuming that a fraction of the 76,000 lbm/sec (equal to the ratio of the area between two cavities to the total open area of the cavity where the rupture occurs) enters the reactor vessel gap. The peak absolute pressure in the reactor vessel gap cavity is 100 psia, and the maximum pressure differential is 100-14.7 = 85.3 psi.

The jet forces from rupture of various pipes is:

Break Location	Jet Force
Primary loop hot let	1800 kips
Primary loop cold leg	1600 kips
Crossover	2250 kips
Steam Line	813 kips
Feedwater line	277 kips

Additional analyses are being performed to determine if additional heat transfer from the steam generator influences the peak pressure differentials. Since the peak compartment pressures occur during the 0.01 sec to 0.3 sec interval it is not expected that steam generator energy additions at 10.0 sec will influence peak compartment pressures.

Structural Design Capability

The compartment differential design pressures as described in Sec 5.9.2 of the Kewaunee FSAR are::

Reactor Cavity (Nozzles)	-	475 psi
Reactor Vessel Gap	-	100 psi
Reactor Steam Generator and Pump Vaults	-	25 psi

The loading from the pressure differentials and the jet forces were used so that the working stress for each structual component affected by the loads would be as given in Table 3.

Other stress levels for both the concrete and steel are presented for comparison in Table 3 to indicate the margin in the design.

TABLE 1 DIMENSIONS OF STEAM GENERATOR VAULT

DESCRIPTIONS		NET VOLUME ft^3	FLOW AREA ft^2
V_v	Steam Generator Vault	19929	
V_a	Base Compartment	66000	
V_b	Foundation Void	1319	
V_c	Containment Vessel	1.32×10^6	
A_{vc}	From Steam Generator Vault to Containment Vessel		329
A_{va}	From Steam Generator Vault to Base Compartment		91
A_{ac}	From Base Compartment To Containment Vessel		113
A_{ab}	From Base Compartment To Foundation Void		1.55

TABLE 2 DIMENSIONS OF THE PENETRATION ANNULI

Penetration Annuli Number		1	2	3	4
V_p	Net Penetration Annulus Volume, $Ft.^3$	117.8	118.7	114.1	117.3
A_{pg}	Net Opening to the Reactor Vessel Gap, $ft.^2$	9.6	10.3	9.6	10.3
A_{pc}		2.9	2.5	2.9	2.5
A_{ps}	Openings to the Containment Vessel, $ft.^2$	12.2	11.2	12	10.7
A_{gc}			7.6		
A_{gt}	Net Opening to the Tube Tunnel, $ft.^2$		6.8		
A_{tc}	Net Opening from the Tube Tunnel to the Containment Vessel, $ft.^2$		33.2		
V_g	Net Volume of the Reactor Vessel Gap, $ft.^3$		223.0		
V_t	Net Volume of the Tube Tunnel, $ft.^3$		4709		

TABLE 3

Load	Stress Levels		
	Concrete		
	Working Stress	Design Stress(f'_c)	Actual Strength
Differential Pressure	1.8 ksi	4.0 ksi	>6.0 ksi
Differential pressure plus Jet force from pipe rupture	3.0 ksi	4.0 ksi	>6.0 ksi
	Steel		
	Working Stress	Yield Stress	Tensile (ultimate) stress
Differential pressure	24 ksi	60 ksi	90 ksi
Differential pressure plus Jet force from pipe rupture	54 ksi	60 ksi	90 ksi

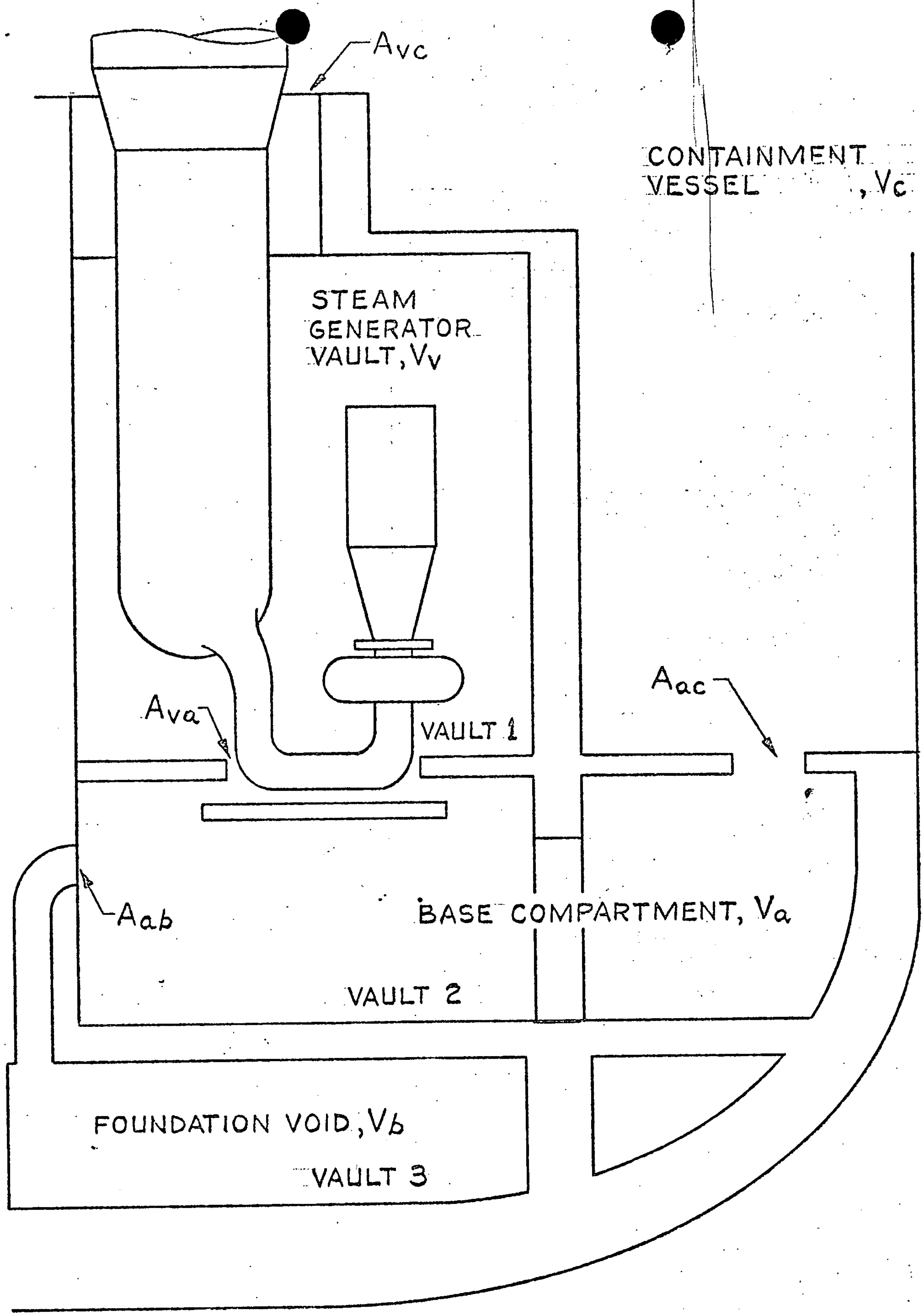

Figure 1 Schematic of Volumes and Flow Areas for pipe rupture in steam generator vault.

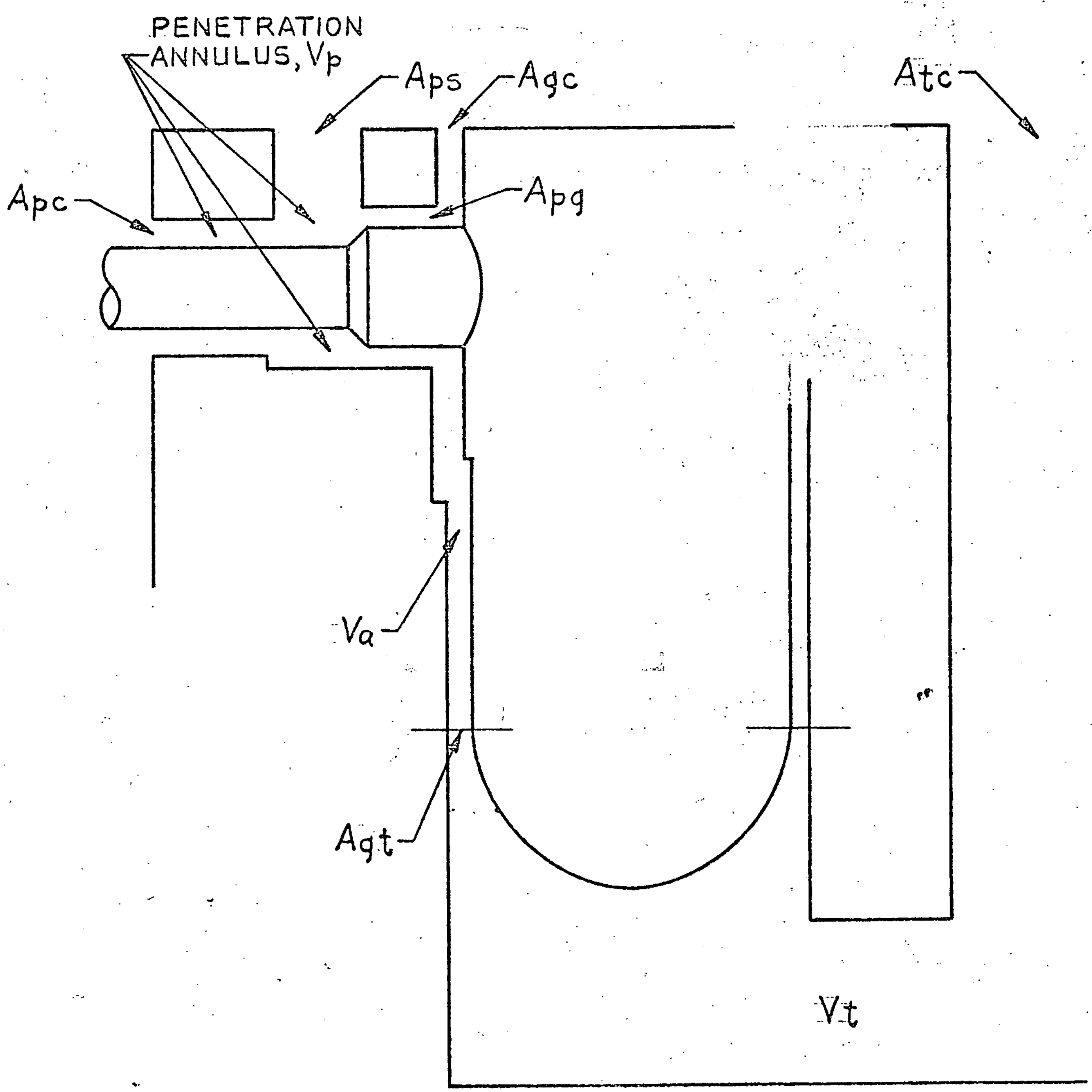

Figure 2 Schematic of Volumes and Flow Areas For pipe rupture in penetration annulus.

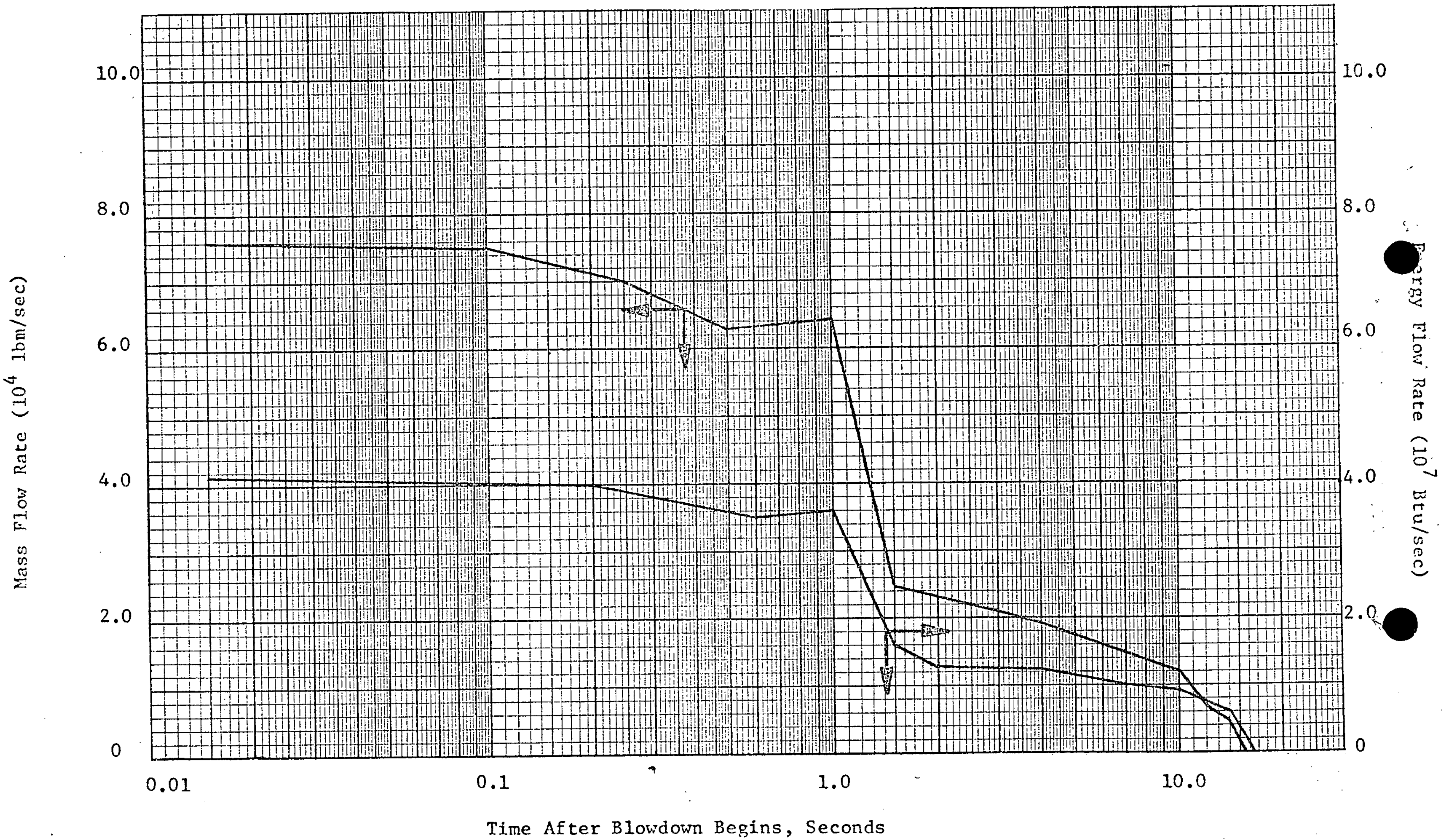

Figure 3. Mass and Energy Blowdown Rates

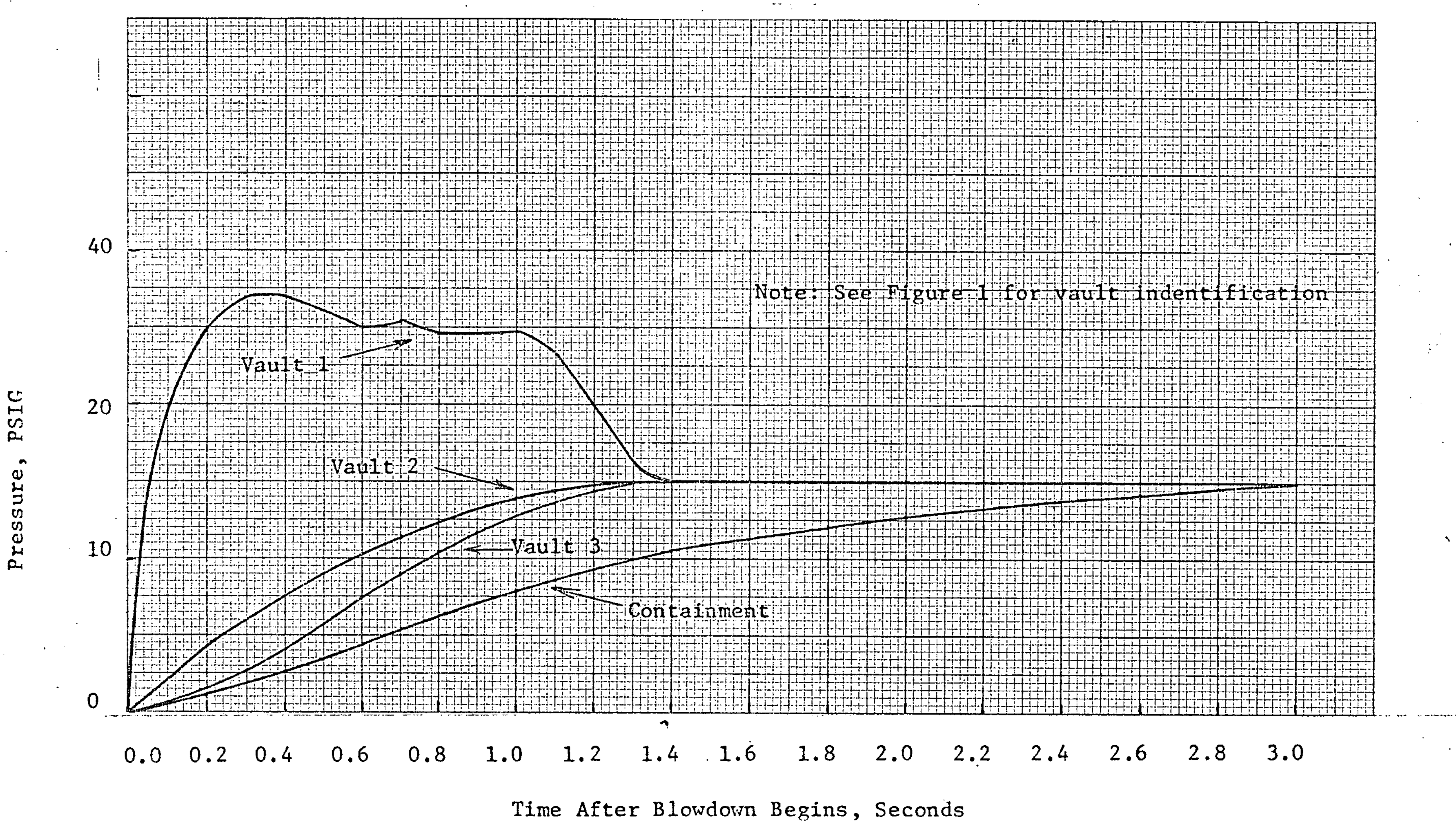

Figure 4. Compartment Pressures